

CuZnSOD deficiency leads to persistent and widespread oxidative damage and hepatocarcinogenesis later in life

Sailaja Elchuri¹, Terry D Oberley^{2,3}, Wenbo Qi⁴, Richard S Eisenstein⁵, L Jackson Roberts⁶, Holly Van Remmen^{4,7}, Charles J Epstein⁸ and Ting-Ting Huang^{*,1,9}

¹Department of Neurology and Neurological Sciences, Stanford University, Stanford, CA 94305, USA; ²Department of Pathology, University of Wisconsin, Madison, WI 53706, USA; ³Pathology Service, VA Hospital, Madison, WI 53705, USA; ⁴Department of Cellular and Structural Biology, UTHSC, San Antonio, TX 78229, USA; ⁵Department of Nutritional Sciences, University of Wisconsin, Madison, WI 53706, USA; ⁶Departments of Pharmacology and Medicine, Vanderbilt University, Nashville, TN 37232, USA; ⁷GRECC, Audie Murphy VA Hospital, San Antonio, TX 78229, USA; ⁸Department of Pediatrics, University of California, San Francisco, CA 94341, USA; ⁹GRECC, Palo Alto VA Health Care System, Palo Alto, CA 94304, USA

Mice deficient in CuZn superoxide dismutase (CuZn-SOD) showed no overt abnormalities during development and early adulthood, but had a reduced lifespan and increased incidence of neoplastic changes in the liver. Greater than 70% of *Sod1*^{-/-} mice developed liver nodules that were either nodular hyperplasia or hepatocellular carcinoma (HCC). Cross-sectional studies with livers collected from *Sod1*^{-/-} and age-matched *+/+* controls revealed extensive oxidative damage in the cytoplasm and, to a lesser extent, in the nucleus and mitochondria from as early as 3 months of age. A marked reduction in cytosolic aconitase, increased levels of 8-oxo dG and *F2-isoprostanes*, and a moderate reduction in glutathione peroxidase activities and porin levels were observed in all age groups of *Sod1*^{-/-} mice examined. There were also age-related reductions in Mn superoxide dismutase activities and carbonic anhydrase III. Parallel to the biochemical changes, there were progressive increases in the DNA repair enzyme APEX1, the cell cycle control proteins cyclin D1 and D3, and the hepatocyte growth factor receptor Met. Increased cell proliferation in the presence of persistent oxidative damage to macromolecules likely contributes to hepatocarcinogenesis later in life.

Oncogene (2005) 24, 367–380. doi:10.1038/sj.onc.1208207
Published online 8 November 2004

Keywords: CuZnSOD; hepatocellular carcinoma; aconitase; 8-oxo dG; cyclin D1; APEX1; Met

Introduction

Hepatocellular carcinoma (HCC) is one of the most common cancers worldwide (Murray and Lopez, 1997;

Levy *et al.*, 2002) and accounts for approximately 84% of all liver cancers. The disease has a very poor prognosis, with greater than 50% of the patients dying within 1 year and only 2–6% surviving for 5 years after diagnosis. Several risk factors for the development of HCC in human population have been identified. A large number of HCC patients have chronic hepatitis B or C infection and liver cirrhosis (Dominguez-Malagon and Gaytan-Graham, 2001). Exposure to aflatoxin B1, alcohol consumption, hemochromatosis, and α -antitrypsin deficiency (Murray and Lopez, 1997; Bonkovsky and Lambrecht, 2000; Perlmutter, 2000; Blum, 2002) are the other major causes of HCC.

Although increased oxidative stress is common among liver diseases that precede the development of liver tumors, the molecular mechanisms of ROS-mediated hepatocarcinogenesis remain poorly understood. Cancer cells usually have low activities of two major antioxidant enzymes, CuZn superoxide dismutase (CuZnSOD) and Mn superoxide dismutase (MnSOD) (Sun *et al.*, 1993; Oberley, 2001), and overexpression of the SODs in transformed cells has been shown to reduce both malignancy and metastatic activity (Oberley, 2001; Zhang *et al.*, 2002). The role of ROS in hepatocarcinogenesis is supported by an electron paramagnetic resonance study on patients with chronic hepatitis and at different stages of malignant transformation (Valgimigli *et al.*, 2002). Several clinical studies with patients at different stages of HCC showed a strong correlation between low levels of SOD and the severity of HCC (Huang and Wu, 1990; Inagaki *et al.*, 1992; Casaril *et al.*, 1994; Liaw *et al.*, 1997), and SOD activities in tumors and surrounding normal tissues have been found to correlate positively with postsurgery survival time in HCC patients (Lin *et al.*, 2001). In addition, overexpression of CuZnSOD in the HCC cell line HepG2 has been shown to suppress cell growth *in vitro* and to reduce tumor mass *in vivo* (Bai *et al.*, 1998). Therefore, CuZnSOD levels may play an important role in the development and prognosis of hepatocarcinogenesis.

CuZnSOD converts superoxide (O_2^-) to H_2O_2 (Fridovich, 1995) and is the major superoxide scavenger

*Correspondence: T-T Huang, Department of Neurology and Neurological Sciences, Stanford University, 3801 Miranda Ave., Bldg 100, Room D3-101, mail stop 154-I, Palo Alto, CA 94304, USA; E-mail: tthuang@stanford.edu

Received 15 June 2004; revised 14 September 2004; accepted 14 September 2004; published online 8 November 2004

in the cytoplasm, nucleus, lysosomes, and intermembrane space of mitochondria (Chang *et al.*, 1988; Keller *et al.*, 1991; Crapo *et al.*, 1992; Sturtz *et al.*, 2001). CuZnSOD (*SOD1*, *Sod1*) transgenic and mutant mice have been widely used to study the role of oxygen free radicals in different experimental systems (Huang *et al.*, 2002; Kruidenier *et al.*, 2003). Increased levels of CuZnSOD usually confer resistance to acute oxidative insults, whereas decreased expression renders mutant mice more sensitive to oxidative stress.

In our investigation of the long-term effects of CuZnSOD deficiency in mutant animals, we observed the development of HCC in congenic *Sod1*^{-/-} mice (*Sod1*^{tm2Cje}) (Huang *et al.*, 1997) on a C57BL/6J (B6) background. The neoplastic transformation ranges from precarcinoma to poorly differentiated HCC, even though the B6 background is known to be resistant to spontaneous and chemically induced hepatocarcinogenesis (Hanigan *et al.*, 1988; Lee *et al.*, 1989, 1991; Pugh and Goldfarb, 1992; Takahashi *et al.*, 2002). In this study, we describe histopathological, biochemical, and gene expression alterations that occur during the course of hepatocarcinogenesis in CuZnSOD mutant mice. Cellular targets known to be sensitive to oxidative damage are affected by CuZnSOD deficiency, and the resulting alterations most likely lead to a disturbance of cellular homeostasis and ultimately to the development of hepatocarcinogenesis later in life.

Results

CuZnSOD mutant mice (Sod1^{-/-}) have a reduced lifespan and develop liver tumors

The mean lifespans for *Sod1*^{+/+}, *-/+*, and *-/-* mice were 29.8 ± 2.1 (mean \pm s.d., $n = 12$), 28.7 ± 1.3 ($n = 12$), and 20.8 ± 0.7 ($n = 18$) months, respectively (Figure 1).

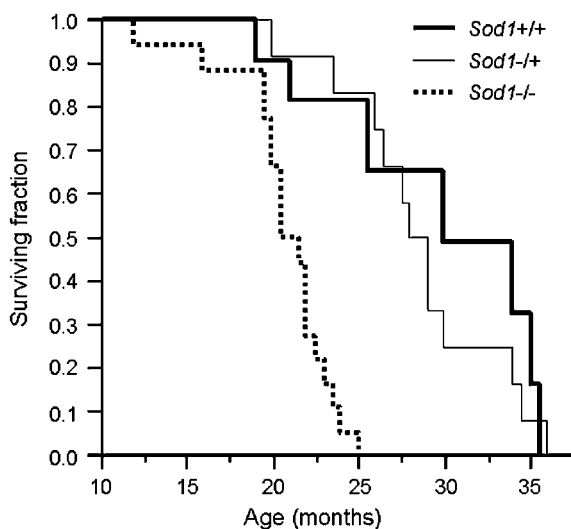


Figure 1 Lifespan analysis of CuZnSOD mutant mice. The life table was analysed by the statistical analysis program JMP using Kaplan-Meier analysis (product limited survival estimate)

There was a significant difference ($P < 0.0001$ by log rank and Wilcoxon) in the survival time between *Sod1*^{-/-} and the control groups (*Sod1*^{-/+} and *+/+*), whereas no significant difference was observed between *Sod1*^{-/+} and *+/+* mice ($P = 0.86$ by log rank and $P = 0.91$ by Wilcoxon).

A high percentage of *Sod1*^{-/-} mice developed liver tumors by 20 months of age (Table 1). Livers collected from *-/-* mice often had multiple visible nodules (> 2 mm in diameter) on the surface or had large outgrowths (> 5 mm in diameter) from the liver. The liver weight to body weight ratios in both male and female *Sod1*^{-/-} mice were significantly higher than those of age-matched *+/+* and *-/+* controls (Table 1). Although male *Sod1*^{-/-} mice appeared to have a higher incidence of liver abnormalities, a contingency χ^2 test failed to show a significant difference between the two genders. Blinded light microscopic examination of a set of three *Sod1*^{+/+} and 15 *Sod1*^{-/-} mice (17.5–23.5 months old) did not reveal any significant pathology in the liver, lung, or kidney of the *Sod1*^{+/+} mice. One *Sod1*^{-/-} mouse showed lymphoma in both the liver and lung (a 23.5 months old female), and a second mouse showed probable lymphoma in the lung only (a 20 months old female). However, all livers from *Sod1*^{-/-} mice showed hepatocyte injury (16–23.5 months, both male and female), which was identified by the presence of hepatocytes that were larger than normal and had enlarged but regular nuclei (Figure 2a). One of 15 *Sod1*^{-/-} livers showed nodular hyperplasia of hepatocytes, and five (both males and females) had HCC (Figure 2b). In HCC, the cells were arranged in either solid nests or in gland-like structures (Figure 2b), and cells and nuclei varied widely in size and shape.

Electron microscopic examination of *Sod1*^{+/+} livers showed the typical ultrastructural features of normal hepatocytes, with one or two medium-sized regular nuclei, an occasional small nucleolus, and a small rim of heterochromatin adjacent to nuclear membranes. The cytoplasm was moderate in amount and showed a moderate number of mitochondria and peroxisomes. Mitochondria were usually elongated, had numerous cristae, and the outer and inner membranes were readily identifiable. Peroxisomes had an electron-dense core and were surrounded by a unit membrane. Rough and smooth endoplasmic reticulum profiles, lipid droplets, and glycogen were identified in small amounts in the cell cytoplasm. The cell surface showed focal microvilli and tight junctions, and rare lipofuscin granules and myelin figures were identified in the cytoplasm. Dead cells were not observed.

In contrast, uninvolved tissue adjacent to tumors in *Sod1*^{-/-} livers showed prominent evidence of cell injury. Nuclei varied in appearance from normal to enlarged nuclei with increased chromatin clumping and more frequent and enlarged nucleoli. The cytoplasm was focally increased in amount, and the number of mitochondria and amount of lipofuscin granules were prominently increased (Figure 2c). Many cells showed prominent myelin figures, both in the cytoplasm and around mitochondria (Figure 2d). Some lipofuscin

Table 1 Incidence of hepatocarcinogenesis in *Sod1* mutant mice^a

| Genotype | Total no. of animals examined | Ratio of liver weight to body weight (% body weight) | | | No. of animals with abnormal appearance of the liver ^b (% total) |
|-----------------|-------------------------------|--|-------------------|--------|---|
| | | Range | Mean | s.e.m. | |
| <i>Sod1</i> +/+ | 10F, 8M | 3.8–9.0 | 6.3 | 0.9 | F, 1/10; M, 0/8 |
| <i>Sod1</i> -/+ | 12F, 11M | 3.8–22.3 | 6.7 | 1.6 | F, 0/12; M, 2 ^c /11 |
| <i>Sod1</i> -/- | 18F | 6.9–19.7 | 12.3 ^d | 1.8 | 10/18 (56%) |
| <i>Sod1</i> -/- | 19M | 6.9–15.0 | 10.5 ^d | 1.0 | 15/19 (79%) |

^aMutant mice (11–29 months of age) were euthanized and autopsied when they became ill. ^bGross appearance of livers showing abnormal nodules. ^cThese two -/+ mice developed HCC at the age of 26 and 29 months. ^dLiver weight to body weight ratio is significantly different from that of +/+ and -/+ controls ($P < 0.05$)

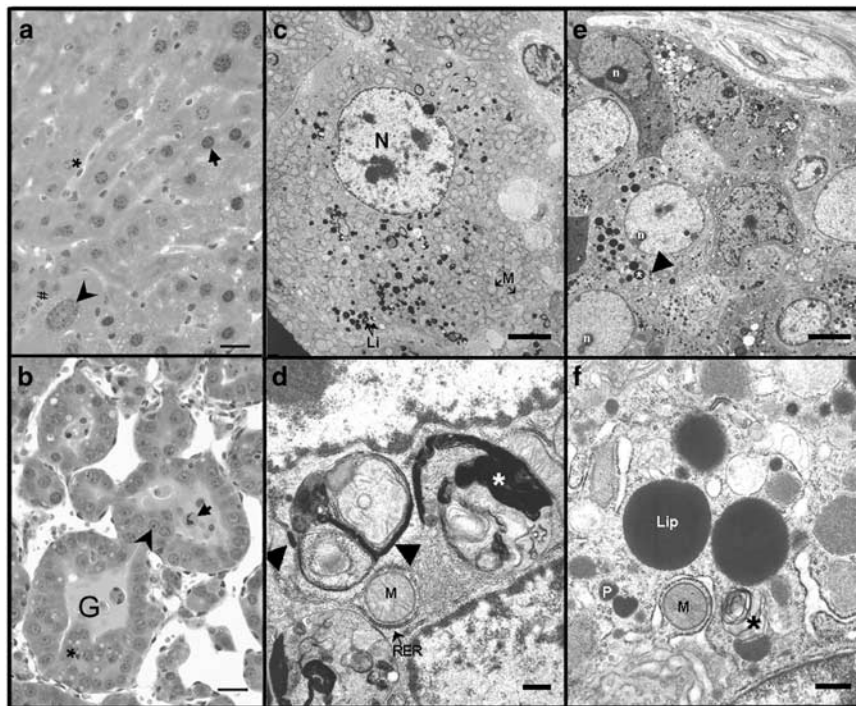


Figure 2 Light and electron microscopy examination of *Sod1*-/- mouse liver. (a) and (b) Light microscopy; (c)–(f) electron microscopy. (a) Hepatocyte injury in uninjured tissue adjacent to HCC. Liver tissue adjacent to HCC shows both normal hepatocytes and injured cells. Normal hepatocytes have round nuclei with moderately dense heterochromatin (arrow) and a moderate amount of cytoplasm. Kupffer cells that are normal in appearance are identified (adjacent to asterisk). Injured hepatocytes were enlarged with large nuclei that had less dense heterochromatin arranged in a stippled pattern (arrowhead) and a large amount of cytoplasm. Neutrophils were often present adjacent to injured hepatocytes (pound symbol is adjacent to a neutrophil). Bar = 25 μ m. (b) HCC. Cells were arranged in solid nests and cords of cells (not shown) and in abnormal glandular structures (G). Nucleoli (arrowhead) were identified in the nuclei. Tumor was often composed of multilayers of cells (asterisk). Dead cancer cells were present in the lumens of glands (arrow). Bar = 25 μ m. (c) Hepatocyte injury in uninjured tissue adjacent to HCC: low magnification. The nucleus (N) was large, with predominant euchromatin and a lesser amount of heterochromatin. Numerous small mitochondria (M) were present in the cell cytoplasm, and lipofuscin (Li) granules were prominent. Bar = 10 μ m. (d) Hepatocyte injury in uninjured tissue adjacent to HCC: high magnification. Normal mitochondria (M) were identified with matrix, cristae, and inner and outer mitochondrial membranes. Mitochondria in liver were often surrounded by rough endoplasmic reticulum (RER). Other mitochondria showed injury, as evidenced by accumulation of electron-dense multilayered myelin-like material adjacent to the outer mitochondrial membrane (arrows). Large amounts of myelin-like material were also present in the cell cytoplasm (asterisk). Bar = 1 μ m. (e) HCC (small cell variant): low magnification. Tumor nuclei often contained nucleoli (n), and mitochondria were few in number. Numerous large (asterisk) and small (arrowhead) electron-dense granules were present in the cytoplasm. Bar = 10 μ m. (f) HCC (small cell variant): high magnification. Occasional mitochondria (M) were identified. Small electron-dense granules surrounded by unit membrane were peroxisomes (P). Large electron-dense granules were lipid droplets (Lip). Only rare disorganized membranes were identified (asterisk). Bar = 1 μ m

appeared to originate in peroxisomes (not shown). Focal cell death was identified, with prominent chromatin condensation, degeneration of cell organelles, and large vacuoles in the cell cytoplasm (not shown).

The tumors in *Sod1*-/- mice were HCCs. They had features of hepatocytes, but with a disorganized arrangement both between cells and within cells (i.e. abnormal cell organelles). The tumor cells were highly

variable in size, from smaller than normal hepatocytes (Figure 2e) to quite large (not shown). Their nuclei were notable for the presence of nucleoli in most cells (Figure 2e). They also varied greatly in size. Similarly, cytoplasmic organelle content was quite variable, depending on the size of the tumor cell; larger tumor cells had more mitochondria and peroxisomes than small ones. All tumor cells had abnormal mitochondria, which were smaller and had more disorganized cristae than normal mitochondria. Some tumor cells had high amounts of glycogen, while others had high amounts of lipid in the cytoplasm (Figure 2f), with occasional tumor cells having crescent-shaped nuclei partially encircling the lipid (not shown). Whereas in small tumor cells, lipofuscin and myelin figures were rare (Figure 2f), in large tumor cells, these were more abundant (not

shown). Intracellular lumens, a diagnostic feature of carcinoma cells, were identified in large tumor cells (not shown).

Other antioxidant enzymes are altered in *Sod1*^{-/-} mice

Enzyme activities were analysed to determine if MnSOD, glutathione peroxidase (GPx), and catalase levels are affected by CuZnSOD deficiency. A 24% increase in MnSOD activity was observed in the liver of *Sod1*^{-/-} mice at 3 and 6 months of age (Figure 3a), but the activity declined to ~70% of the control level in the end-stage animals. On the other hand, GPx activities were already reduced by 40% in *Sod1*^{-/-} mice at 3 months of age and were further diminished as the mice aged or became ill (Figure 3b). No change in catalase

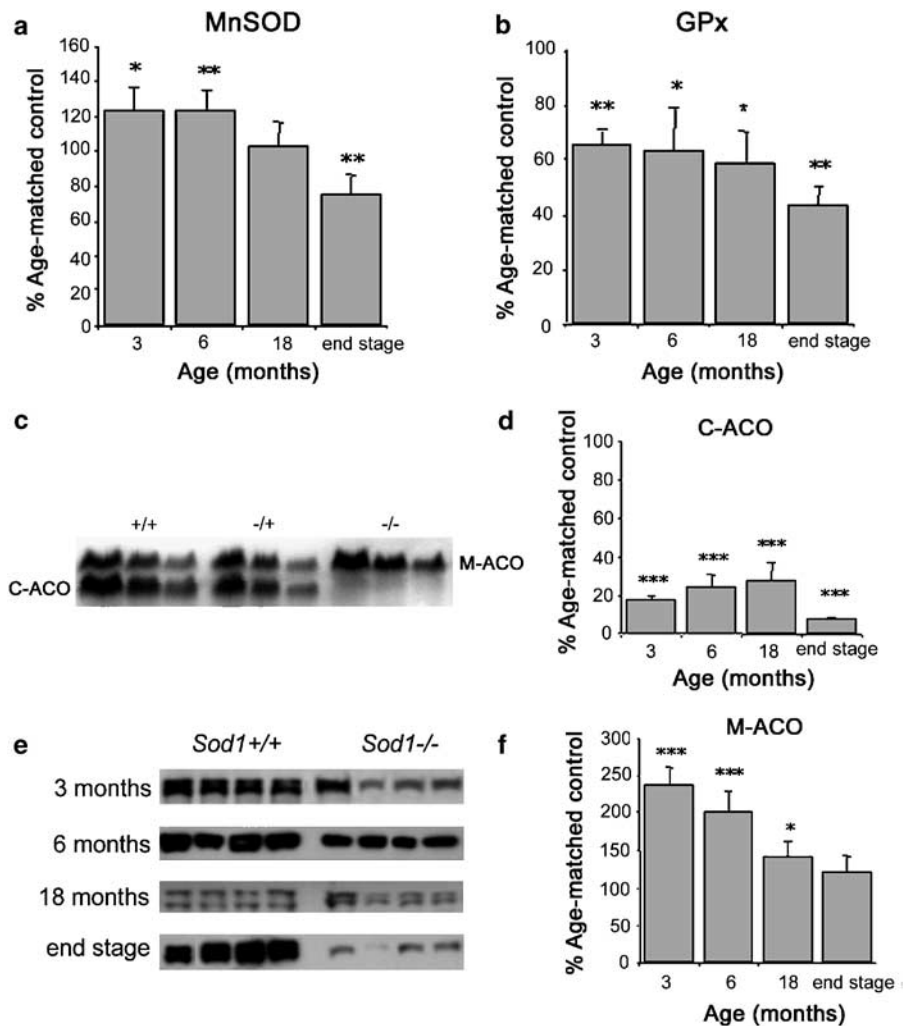


Figure 3 MnSOD, GPx, and aconitase levels in the livers of *Sod1*^{-/-} mice. (a) MnSOD and (b) GPx enzyme activities. Five independent samples of each genotype and age were analysed. (c) Separation and detection of C-ACO and M-ACO activities by cellulose gel. Each set of three lanes represents the serial dilution of a single sample. (d) C-ACO activities expressed as the percentage of age-matched control. Sample size: 3 and 6 months, $n = 5$ each; 18 months, $n = 5$ for *Sod1*^{+/+} and $n = 7$ for *Sod1*^{-/-}; end-stage, $n = 5$ for the age-matched *Sod1*^{+/+} and $n = 11$ for *Sod1*^{-/-} samples. (e) C-ACO protein levels determined by Western blot analyses. Representative results from four each *Sod1*^{+/+} and *Sod1*^{-/-} mice of different ages are shown. (f) M-ACO activities expressed as the percentage of age-matched controls. Sample size was the same as that of C-ACO analyses. * $P \leq 0.05$; *** $P \leq 0.001$

activities was observed in any age group examined (data not shown). In contrast to the age-related changes in MnSOD activities, no reduction in MnSOD protein levels was observed in older *Sod1*^{-/-} mice (data not shown). Consistent with the protein levels, no age-related changes in MnSOD message levels were detected by RT-PCR analysis (Supplementary data and Supplementary Table). These results suggested that the changes in MnSOD activity were caused by post-translational modifications. Similarly, no alteration in GPx message levels was observed (Supplementary data).

Widespread oxidative damage in the liver of Sod1^{-/-} mice

Several assays were carried out to determine the level of steady-state oxidative damage in the liver of *Sod1*^{-/-} mice. These included measurements of aconitase activities, protein oxidation, lipid peroxidation, and oxidative DNA damage. The activity of aconitase has been used as an indicator for superoxide-induced damage because of its sensitivity to direct inactivation by superoxide radicals (Gardner, 1997). Therefore, cytosolic (C-ACO) and mitochondrial (M-ACO) aconitase activities were determined to assess the extent of oxidative damage in the cytoplasmic and mitochondrial compartments, respectively. A 72% reduction in C-ACO activity was observed in *Sod1*^{-/-} mice at as early as 3 months of age, and the reduction was similar across all age groups examined (Figure 3c and d). Consistent with the reduced enzyme activities, Western blot analyses showed a greater than fourfold reduction of C-ACO protein in all *Sod1*^{-/-} livers examined. Moreover, C-ACO was almost undetectable in some end-stage samples (Figure 3e). However, the reduction in protein was not due to a decrease at the transcriptional level, as RT-PCR analysis showed a normal level of C-ACO message in *Sod1*^{-/-} liver in all age groups examined (Supplementary data). Again, the data suggest that post-translational modification may play a role in the marked reduction of C-ACO.

In contrast to the reduction in C-ACO, an increase in M-ACO activity was observed in the livers of *Sod1*^{-/-} mice at 3 months of age (Figure 3c and f). However, the activity gradually declined as the mice aged or became ill (Figure 3f). Unlike activity, M-ACO protein levels remained unaltered in the *Sod1*^{-/-} livers at all age groups examined (data not shown). Thus, the increased M-ACO activity was likely, in part, due to an increase in MnSOD activity (Figure 3a), which had been shown to reduce the rate of M-ACO inactivation (Gardner *et al.*, 1995). To determine if there was a change in mitochondrial content in response to the elevated oxidative stress, the mitochondrial structural protein, porin, was used as a marker. A 20–30% reduction in porin levels was detected in the livers of all age groups examined (Supplementary data).

To assess the overall level of oxidative modification of proteins in the liver of *Sod1*^{-/-} mice, we carried out Western blot analyses using the OxyBlot™ Oxidized Protein Detection Kit. A consistent increase in protein

oxidation was detected only in the end-stage samples (Figure 4a), suggesting that protein oxidation is not a prominent feature in *Sod1*^{-/-} mice until they reach the diseased state. Interestingly, a 30 kDa protein was prominently oxidized in both +/+ and -/- samples, and the protein gradually became undetectable in -/- samples as the mice aged (Figure 4a). The protein was subsequently identified by mass spectral analysis as carbonic anhydrase III (CAIII) (data not shown), which is known to be abundant in the liver and to be very sensitive to oxidative modification (Cabiscol and Levine, 1995). Western blot analysis using a specific antibody against CAIII showed an age-associated decrease in the livers of *Sod1*^{-/-} mice, which explained the disappearance of the 30 kDa protein in Oxyblot in older *Sod1*^{-/-} mice (Figure 4a and b). Furthermore, the reduction in protein levels was coupled to a marked reduction of CAIII mRNA in older *Sod1*^{-/-} mice (Supplementary data). These results suggest that the expression of CAIII is affected at the transcriptional level under the condition of CuZnSOD deficiency. No age-related reduction in CAIII was detected in healthy *Sod1*^{+/+} controls up to 18 months of age (data not shown).

To determine the extent of lipid peroxidation in the livers of *Sod1*^{-/-} mice, levels of malondialdehyde (MDA), 4-hydroxyalkenals (HAE), and F2-isoprostanes were measured. Whereas a 2.2- and 2.7-fold increase in MDA was observed in 18-month and end-stage *Sod1*^{-/-} livers, respectively (Figure 4c), no change in HAE levels was observed (data not shown). On the other hand, F2-isoprostanes analysis revealed a 30–60% increase in all *Sod1*^{-/-} samples examined (Figure 4d).

To determine if there was an increase in oxidative DNA damage, 8-oxo dG were determined in total DNA extracted from the livers of *Sod1*^{-/-} and age-matched controls. A roughly twofold increase in 8-oxo dG level was observed in *Sod1*^{-/-} mice in all age groups examined (Figure 5a). Immunohistochemical (IHC) analysis of *Sod1*^{+/+} and *-/- liver sections using an antibody that recognizes both 8-oxo dG and 8-oxo G revealed strong staining signals in the nuclei, which disappeared with DNase I pretreatment (Figure 5b). However, it is likely that oxidized RNA and mitochondrial DNA also exist, especially in the *Sod1*^{-/-} livers, as the staining intensities in the cytosol were always stronger with RNase A or DNase I pretreatment than that in the controls without primary antibody. APEX1 is the major AP endonuclease for repairing oxidative DNA damage. To determine if increased oxidative DNA damage is correlated with alterations in APEX1, Western blot analyses were carried out. Whereas a decrease in APEX1 was observed in the livers of 3-month-old *Sod1*^{-/-} mice (Figure 5c), a progressive increase was observed in 6- and 18-month-old *Sod1*^{-/-} mice (Figure 5c). RT-PCR analysis also revealed an increase in the level of APEX1 message at 6 months of age (Supplementary data). IHC analysis of APEX1 showed a strong nuclear-staining pattern in *Sod1*^{-/-} sections and a weaker staining pattern in *Sod1*^{+/+} sections (Figure 5d).*

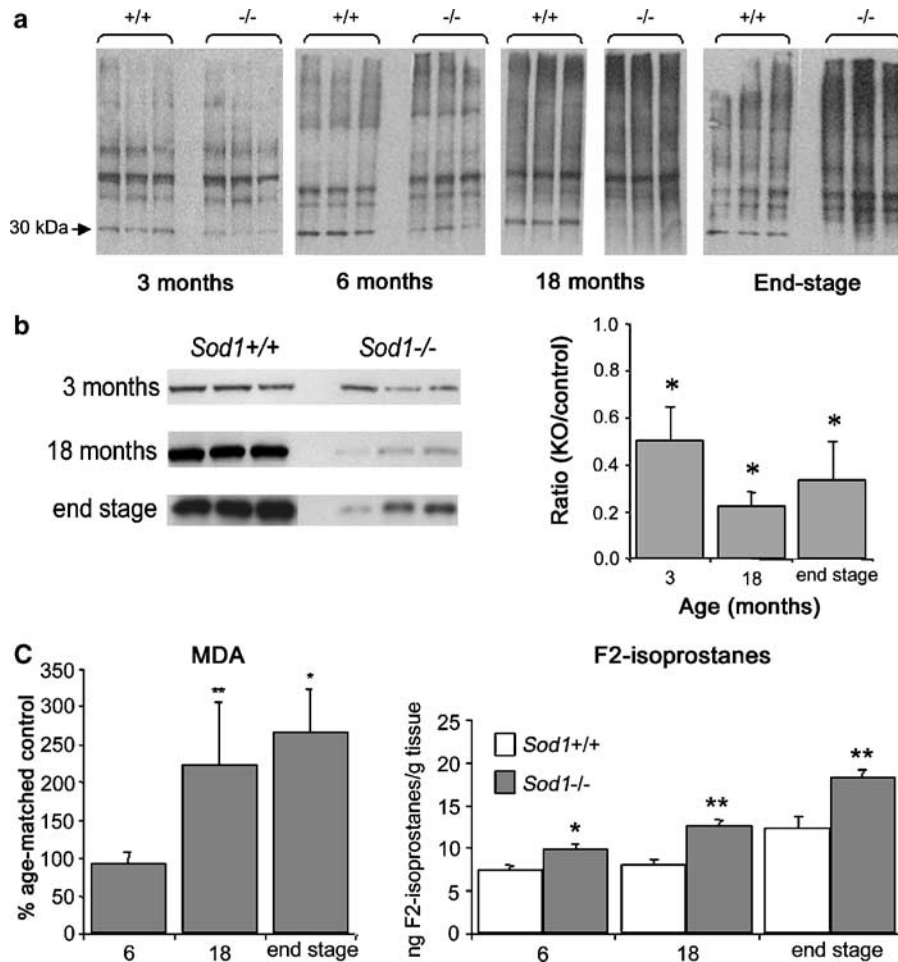


Figure 4 Oxidative modification of proteins and lipids. (a) Oxyblot analyses. DNP-derivatized liver tissue lysates were analysed for the presence of oxidized protein. The 30 kDa protein became undetectable in 18 months and end-stage *Sod1*^{-/-} samples. (b) CAIII levels determined by Western blot analyses (left panel) and quantified by normalization to the levels of actin (right panel). A minimum of five independent samples each were analysed; representative results from three each *Sod1*^{+/+} and ^{-/-} mice of different ages are shown. (c) MDA levels. The *Sod1*^{-/-} levels were normalized to that of age-matched controls. F2-isoprostanes levels. Five independent samples each were analysed for lipid peroxidation markers. **P* ≤ 0.05; ***P* ≤ 0.01

Increased levels of cyclin D1, D3, and Met were observed in *Sod1*^{-/-} mice

To assess possible changes in the markers known to associate with the development of HCC in mouse models, we analysed the levels of the cell cycle control proteins cyclin D1, D2, and D3, and the hepatocyte growth factor receptor Met by Western blot analyses. Whereas there was a consistent upregulation of cyclin D1 and D3 in most *Sod1*^{-/-} samples starting at 6 months of age (Figure 6a), no consistent change in cyclin D2 was observed (data not shown). Similarly, an increase in Met (Figure 6b) was found in 6- and 18-month samples. However, no statistically significant changes in message levels were observed for cyclin D1 and Met (Supplementary data). The alterations of cyclins D1 and D3 and of Met may represent early events in the course of hepatocarcinogenesis in *Sod1*^{-/-} mice.

Discussion

Sod1^{-/-} is a new animal model for hepatocarcinogenesis. Congenic *Sod1*^{-/-} mice on a C57BL/6J background have an increased incidence of spontaneous liver tumors and a reduced lifespan. All showed hepatocyte injury and greater than 30% developed HCC by 20 months of age. This number is an underestimate since we did not serially section liver samples and, in fact, gross examination showed that approximately 70% of the mice developed tumor nodules. The time course and the frequency of tumor development in *Sod1*^{-/-} mice are comparable to that of the other mouse models of HCC (Chisari *et al.*, 1989; Yu *et al.*, 1999; Moriya *et al.*, 2001). Widespread oxidative damage was detected in the liver in the cytoplasm and nucleus, and the effects ranged from gene dysregulation to protein inactivation. C57BL/6 (B6) mice are known to be resistant to the development of spontaneous and chemically induced

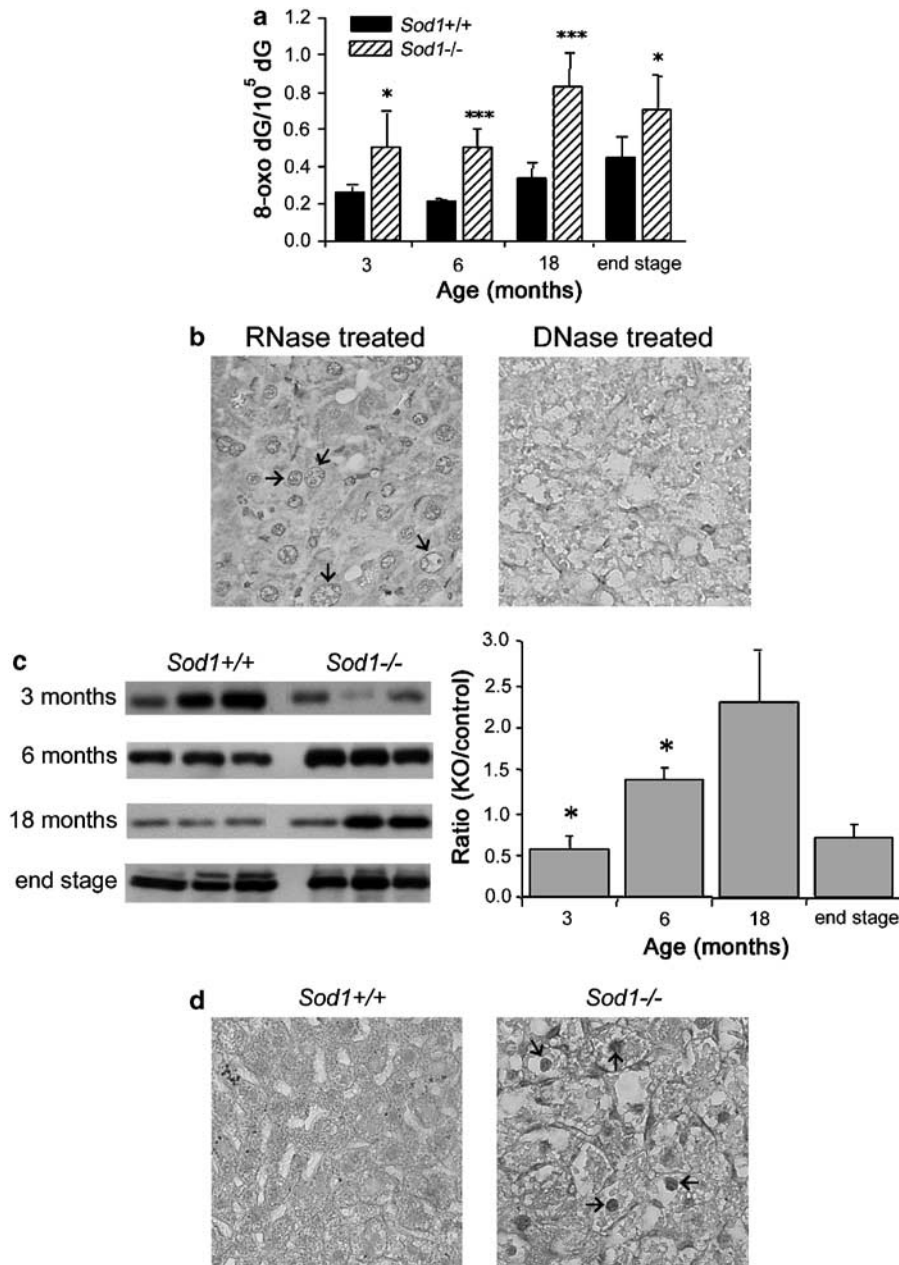


Figure 5 8-oxo dG and APEX1 levels in *Sod1*^{-/-} mice. **(a)** 8-oxo dG levels determined by HPLC-EC analyses. Sample size: 3, 6, and 18 months, *n* = 5 each; end-stage, *n* = 12 for *Sod1*^{-/-} and *n* = 10 for *Sod1*^{+/+}. **(b)** IHC analysis of 8-oxo dG. The signal intensities were strong in the nuclei (left panel, arrows), and were sensitive to DNase I pretreatment (right panel). Three *Sod1*^{+/+} and six *Sod1*^{-/-} liver sections from 18-month-old mice were analysed; representative sections are shown. **(c)** APEX1 protein levels determined by Western blot analyses (left panel) and quantified by normalization to the levels of actin (right panel). A minimum of five independent samples each were analysed; representative results from three each *Sod1*^{+/+} and *-/-* mice of different ages are shown. **P* ≤ 0.05; ****P* ≤ 0.001. **(d)** IHC analysis of APEX1. *Sod1*^{-/-} liver sections showed a strong nuclear-staining pattern (arrows), while *Sod1*^{+/+} sections showed a weaker nuclear-staining pattern. Five *Sod1*^{+/+} and 7 *Sod1*^{-/-} liver sections from 18-month-old mice were analysed; representative sections are shown

HCC (Hanigan *et al.*, 1988; Lee *et al.*, 1989, 1991; Pugh and Goldfarb, 1992; Takahashi *et al.*, 2002). However, with a single gene mutation leading to CuZnSOD deficiency, a high percentage of *Sod1*^{-/-} mice on B6 background developed neoplastic changes in the liver. This suggests that the condition of CuZnSOD deficiency

can be both a potent initiator and promoter in hepatocarcinogenesis.

CuZnSOD is located throughout the cell in all subcellular locations except the inner mitochondrial membrane and the mitochondrial matrix. Our ultrastructural analysis of *Sod1*^{-/-} livers provides strong

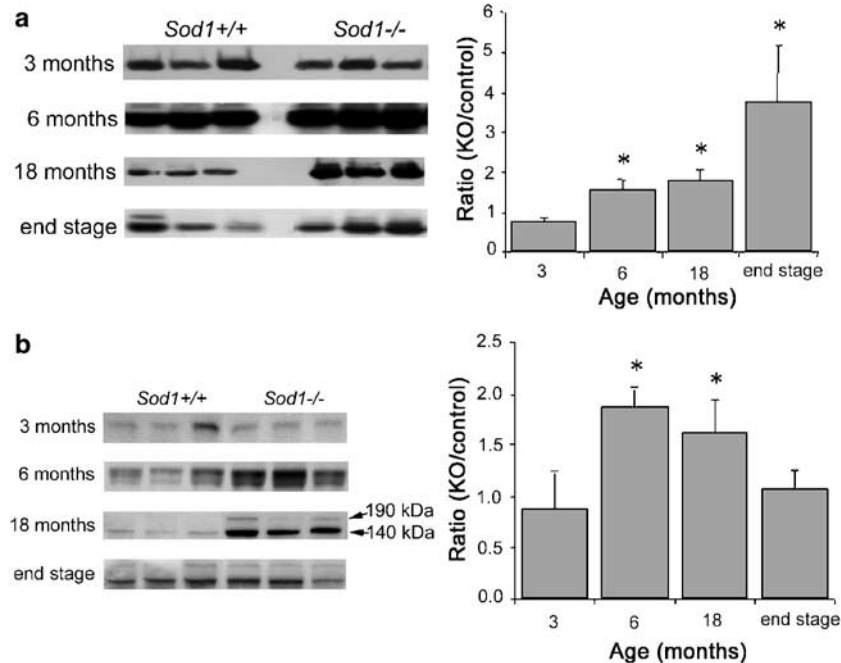


Figure 6 Western blot detections of cyclin D1 and Met. (a) Cyclin D1. Cyclin D3 shows a similar profile as that of cyclin D1; therefore, the data are not presented here. (b) Met. The 190 kDa protein was visible in some of the 18-month-old *Sod1*^{-/-} samples. Protein levels of cyclin D1 and Met were determined by Western blot analyses (left panel) and quantified by normalization to the levels of actin (right panel). A minimum of five independent samples each were analysed; representative results from three each *Sod1*^{+/+} and ^{-/-} mice of different ages are shown. **P* ≤ 0.05

evidence of membrane injury, with myelin figures prominent around mitochondria and in the cytoplasm. Our studies also provide strong evidence for lipid peroxidation, since lipofuscin, a morphologic marker of lipid peroxidation (Oberley *et al.*, 2000), was detected in the cytoplasm and in peroxisomes. Direct measurement of lipid peroxidation markers in *Sod1*^{-/-} liver also showed a consistent increase in MDA and F2-isoprostanes (Figure 4c). Nuclear injury was present and chromatin was focally clumped and nuclei and nucleoli were focally enlarged. Hepatocytes from wild-type mice at this same age did not demonstrate these changes.

Tumor cells in *Sod1*^{-/-} mice had the features of HCC, with abnormal nuclei with frequent nucleoli, numerous mitochondria and peroxisomes, glycogen, lipid, rough and smooth endoplasmic reticulum, and tight junctions, but these features were disorganized, illustrating the principle that cancer cells are a caricature of normal cells. HCC was not observed in wild-type mice. Lipofuscin was only identified in tumor cells with a large number of cell organelles (e.g. mitochondria and peroxisomes), a finding in agreement with a previous study that demonstrated increased lipid peroxidation only in renal cancer cells with large numbers of mitochondria (Oberley *et al.*, 1999).

Oxidative stress has a wide spectrum of effects on gene regulation, protein activities, and nucleic acid integrity. C-ACO and M-ACO have been used as sensitive biomarkers for increased oxidative stress because their [4Fe-4S] clusters, which are required for

enzymatic activity, are accessible to low molecular weight compounds including agents that disrupt Fe-S clusters such as O₂⁻, NO, ONOO⁻, and OH[•] (Drapier, 1997; Gardner, 1997; Eisenstein, 2000). In the case of C-ACO, interest has focused on the role of such agents in promoting loss of the Fe-S cluster and possible conversion of the protein to iron regulatory protein 1 (IRP1), which post-transcriptionally regulates the synthesis of proteins required for the maintenance of iron homeostasis. The [4Fe-4S] cluster of the aconitases can be partially or completely removed by various cluster perturbants, and the evidence indicates that this is likely a complicated multistep process (Kennedy and Beinert, 1988; Kennedy *et al.*, 1997).

In the case of O₂⁻, direct attack on the [4Fe-4S] cluster of purified C-ACO leads to loss of the one iron not directly ligated to the protein, thereby generating the (3Fe-4S) form of the protein, which lacks both aconitase and RNA binding activity (Flint *et al.*, 1993). However, recent studies in *Drosophila* lacking SOD1 revealed an increase in IRP1 RNA binding activity, suggesting an ability of O₂⁻ to promote complete loss of the [4Fe-4S] (Missirlis *et al.*, 2003). An equally plausible scenario is that O₂⁻ also interferes with the pathway of cytosolic Fe-S assembly. Some protein participants in the pathways of Fe-S cluster assembly, such as iscU (iron-sulfur cluster), have a transient Fe-S cluster, which is donated to targeted apo Fe-S proteins. Interestingly, the Fe-S cluster in iscU is similar to that in the aconitases in that it is solvent

accessible (Agar *et al.*, 2000), suggesting that O_2^- and other cluster perturbants may impair the function of pathways of Fe-S cluster assembly and possibly repairs. Our finding that IRP1/C-ACO protein level is greatly reduced in *Sod1*^{-/-} animals suggests that interference with cluster assembly/disassembly leads to degradation of the C-ACO form on oxidative removal of the Fe-S cluster or to altered synthesis or degradation of the apo or IRP1 form of the protein if Fe-S assembly pathway is disrupted (Crawford *et al.*, 1998; Haddow *et al.*, 2003). Interestingly, IRP1/C-ACO protein is reduced in the liver of patients with severe iron overload caused by hemochromatosis (Neonaki *et al.*, 2002), further indicating that oxidative stress influences IRP1/C-ACO function at multiple levels.

In contrast, M-ACO protein levels were not affected, and activity was only reduced in the later stages. However, measurements on the mitochondrial content of *Sod1*^{-/-} livers using porin as a marker showed a moderate reduction in porin levels. These data suggest that oxidative damage is relatively mild in the mitochondrion. Since increased mitochondrial DNA mutation and alterations in mitochondrial DNA copy number are frequently observed in malignant tissues (Lee *et al.*, 2004), it would be important to determine the extent of changes in mitochondrial DNA in future studies. MnSOD and GPx are both sensitive to inactivation by various oxygen free radicals (Pigeolet *et al.*, 1990; Asahi *et al.*, 1995). Whereas GPx already showed a reduction in activity at 3 months of age, MnSOD showed an increase in activity at this early stage (Figure 3a and b). Since GPx is located in the cytosol and mitochondria, while MnSOD is only located in the mitochondria (Muse *et al.*, 1994), the differences in subcellular localization may help to explain the different outcomes between these two enzymes. The age-related decrease in activities without a significant decrease in protein or message again suggests that the effects of oxidative damage are at the protein level and that there is a progressive increase in oxidative damage with age in the liver of *Sod1*^{-/-} mice. The lack of decrease in MnSOD protein levels suggests that oxidative damage to MnSOD may not have triggered proteolytic degradation to remove the inactivated enzyme. Whether this has to do with the mitochondrial localization of MnSOD remains to be determined.

The persistent increase in 8-oxo dG levels in *Sod1*^{-/-} mice suggests increased oxidative damage in the nucleus and mitochondria. The oxidized DNA base, 8-oxo dG, is known to cause GC→AT transversions (Olinski *et al.*, 2002; Wallace, 2002), leading to increased DNA mutation. It is well established that increased DNA mutation and genomic instability predisposes cells and tissues to accelerated senescence and neoplastic transformation (Nowell *et al.*, 1979; Loeb, 1991). Therefore, increased oxidative DNA damage is of particular importance, as it provides the opportunity for DNA mutation and ultimately genomic instability to occur. The dual-function protein APEX1 is responsible for repairing certain oxidative DNA damage and for the activation of redox-sensitive transcription factors such

as c-Jun and c-Fos (Evans *et al.*, 2000). Decreased expression of APEX1 is associated with increased cellular sensitivity to oxidative stress and genomic instability (Ozaki *et al.*, 2002), while increased as well as ectopic expression of APEX1 is associated with a number of carcinomas (Bobola *et al.*, 2001; Puglisi *et al.*, 2001; Robertson *et al.*, 2001). The expression pattern of APEX1 in *Sod1*^{-/-} mice suggested a decreased expression at 3 months of age and an increased expression in older mice, with the increase mainly in the nuclei. The data suggest that the upregulation of APEX1 in older *Sod1*^{-/-} mice is in response to increased oxidative DNA damage in the nuclei.

It was surprising that an increased protein carbonyl content was observed only in end-stage *Sod1*^{-/-} mice, while other indices of oxidative damage appeared much earlier. Since oxidized proteins are often recognized and degraded by proteosomes (Shringarpure *et al.*, 2001), it is possible that oxidized proteins are quickly degraded in the liver of *Sod1*^{-/-} mice and only have a chance to accumulate to a significant amount when the animals become ill. Accumulation of oxidized proteins in older *Sod1*^{-/-} mice may lead to alterations in cellular homeostasis (Levine, 2002; Shringarpure and Davies, 2002) and add further insult to the already dysfunctional hepatic tissue. Furthermore, although the ROS-sensitive CAIII protein was prominently oxidized in both *Sod1*^{+/+} and *-/-* mice, CAIII protein and message levels showed clear age-related decreases in the liver of only *Sod1*^{-/-} mice; no obvious age-related decreases were detected in healthy *Sod1*^{+/+} mice. CAIII has been shown to be sensitive to oxidative modification, and a marked reduction in CAIII was observed in the livers of Fischer 344 rats (Cabiscol and Levine, 1995) by 20 months of age. The function of CAIII, as well as other carbonic anhydrases within the family, is to catalyze the interconversion between CO₂ and HCO₃⁻ to maintain acid-base balance in tissues. CAIII has two sulfhydryl groups and has been suggested to play a role in scavenging oxygen radicals in cells (Lii *et al.*, 1994; Raisanen *et al.*, 1999). A recent survey of the activities and protein and message levels of CAI, II, and III in 60 HCC patients showed a consistent reduction within the tumors in comparison to the corresponding adjacent normal liver tissues (Kuo *et al.*, 2003). Accordingly, it is possible that CAIII level is lower in the liver tumor than in the adjacent normal tissue in *Sod1*^{-/-} mice.

Oxidative DNA damage in S phase poses problems to replicating cells. Cells attempting to duplicate damaged DNA templates are more likely to undergo deleterious genetic changes that may foster the onset of genomic instability and cancer. Loss of cell cycle regulation would be expected to exacerbate such adverse consequences. Higher levels of cyclin D1 became apparent by 6 months of age in *Sod1*^{-/-} mice, and the level increased progressively with age. A similar trend was also observed in cyclin D3, suggesting that these two proteins are coregulated in *Sod1*^{-/-} livers. The progressive increase in cyclin D1 and D3 levels may be a response to increased cell proliferation resulting from increased cell damage and death under conditions of

CuZnSOD deficiency. Conversely, increased cyclin D1 and D3 may be responsive to elevated ROS, which stimulate cell proliferation (Liu and Liu, 2004; Sauer *et al.*, 2004). The increase in ROS may have caused an increase in cell cycle progression and subsequently contributed to hepatocarcinogenesis in *Sod1*^{-/-} mice. Consistent with this hypothesis, overexpression of cyclin D1 in transgenic mice leads to the development of HCC by 15–17 months of age (Deane *et al.*, 2001). The discrepancy between cyclin D1 mRNA and protein levels suggests that there are regulatory mechanisms acting at the post-transcriptional level, which have been observed in NIH 3T3 cells (Rosenwald *et al.*, 1995) and in human lymphoid malignancies (Sola *et al.*, 1999). Parallel to the upregulation of cell cycle proteins, higher levels of the hepatocyte growth factor receptor, Met, was observed in 6- and 18-month-old *Sod1*^{-/-} samples. The increase may lead to dysregulation of Met signaling and increased cell proliferation and neoplastic changes. Transgenic mice overexpressing Met have been shown to develop early HCC (Wang *et al.*, 2001), and a withdrawal of Met overexpression leads to a complete remission of HCC. The level of Met mRNA remained unaltered in *Sod1*^{-/-} animals, suggesting that Met protein is increased by a post-transcriptional regulation.

Although CuZnSOD deficiency is ubiquitous in *Sod1*^{-/-} mice, spontaneous tumors are only observed in the liver. This selectivity may have to do with the special environment and the characteristics of the hepatic tissue. Liver is the major organ for xenobiotic metabolism (Anzenbacher and Anzenbacherova, 2001; Jaeschke *et al.*, 2002) and is also the major organ for iron transport and storage (Crichton *et al.*, 2002; Fletcher and Halliday, 2002). As a result, large amounts of oxygen free radicals are constantly being generated in this environment. To protect liver from the harmful effects of the toxic by-products, high levels of antioxidant enzymes are present. There is roughly 10 times more CuZnSOD and 10 to 20 times more catalase activity in the liver than in the heart, lung, skeletal muscle, and brain (TT Huang, unpublished data). Liver also has a tremendous capacity for regeneration, and can grow back to its original size with as much as 70% of the mass removed (Court *et al.*, 2002; Diehl, 2002; Zimmermann, 2002). It is likely that high-level ROS generation makes liver susceptible to perturbations in antioxidant levels, and the high capacity for regeneration provides the opportunity to select for cells with replication advantage for clonal expansion.

Based on the findings presented in this study, we propose (Figure 7) that CuZnSOD deficiency in the liver leads to damage to macromolecules such as DNA, proteins, and lipids. This in turn leads to cell injury and cell death, which cause the otherwise dormant hepatocytes to reenter the cell cycle for regeneration. At the same time, redox-sensitive proteins and transcription factors are activated in response to the increased oxidative stress, leading to increased gene transcription and cell proliferation. Continuous damage to DNA and other macromolecules coupled with increased cell proliferation increases the probability of DNA mutation

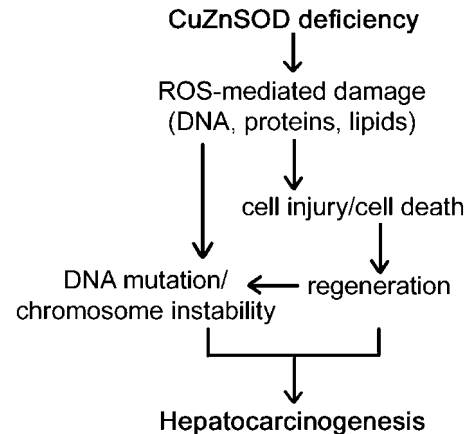


Figure 7 Diagram depicting the proposed sequence of events leading to hepatocarcinogenesis due to CuZnSOD deficiency

and genomic instability, which in the long run leads to hepatocarcinogenesis.

Materials and methods

Generation and monitoring of *Sod1*^{-/-} mice

Sod1^{-/-} mice and the corresponding ^{-/+} and ^{+/+} controls were generated from the intercross between congenic B6 < *Sod1*^{-/+} > C57BL/6 mice (N12) (Huang *et al.*, 1997). All mice were housed in the pathogen-free facility at UC San Francisco (UCSF) and the Palo Alto VA Health Care System, and were fed sterilized LabDiet® 5001 (4.5% fat, PMI Nutrition Intl. Inc., Brentwood, MO, USA) from weaning. The mice were maintained on a 12-h light/dark cycle, at a constant temperature between 20 and 22°C and were given food and water *ad libitum*. Mice were checked daily by animal care personnel and weekly by veterinary nurses. All animal handling procedures were carried out according to the protocols approved by the Committee on Animal Research at UCSF and the Subcommittee on Animal Studies at the Palo Alto VA Health Care System.

To determine lifespan, 12 *Sod1*^{+/+} (8M, 4F), 12 *Sod1*^{-/+} (7M, 5F), and 18 *Sod1*^{-/-} (9M, 9F) mice were used. To characterize the biochemical changes that occur before and during the development of HCC, cross-sectional studies were carried out with tissues from ages 3, 6, and 16–18 months. In addition, tissues from a group of *Sod1*^{-/-} mice were collected when the mice became ill and had to be euthanized. These mice were labeled as ‘end-stage’ and ranged in age from 11 to 23 months. Tissues from a small number of age-matched ^{+/+} mice were collected as controls for the ‘end-stage’ ^{-/-} samples.

Collection and processing of tissues

At the specified ages, or when they became ill, the mice were euthanized with an overdose of pentobarbital (0.5 mg/g body weight). All tissues were sequentially removed and processed for histopathology, biochemical, molecular biology, and Western blot analyses. A minimum of five independent samples for each genotype/age was used for the quantitative assays and Western blotting.

For biochemical and Western blot analyses, livers were homogenized in three volumes ($w:v=1:3$) of lysis buffer containing 50 mM Tris-HCl (pH 8.0), 0.6 mM $MnCl_2$, 2 mM citric acid, and the Complete Protease Inhibitor Cocktail (Roche, Indianapolis, IN, USA). Citric acid was used in the lysis buffer to protect aconitases from oxidative inactivation (Gardner and Fridovich, 1991). The concentration of citric acid used did not interfere with other enzyme activities (data not shown). The tissue lysates were freeze-thawed three times between liquid nitrogen and room temperature water to disrupt the mitochondrial membrane. Tissue lysates were centrifuged at 10 000 g at 4°C for 10 min. The supernatants were removed for the determination of protein concentration (BCA protein assay, Pierce, Rockford, IL, USA) and aliquoted for storage at -80°C.

Histopathology assessment

At the time of dissection, body weight, liver weight, and the gross morphology of the liver were recorded. For histopathological analysis, the liver, lung, and kidney were cut into small pieces and fixed overnight in 10% neutral-buffered formalin (Fisher Scientific, Pittsburgh, PA, USA) before transfer to 70% ethanol. Paraffin-embedded tissues were sectioned at 5 μm and stained with hematoxylin and eosin (H&E) for examination under the light microscope. For an unbiased assessment of the histopathological changes in *Sod1*^{-/-} mice, H&E sections from three *Sod1*^{+/+} (three male, age 17.5–18 months) and 15 *Sod1*^{-/-} mice (eight male, seven female; age 17.5–23.5 months) were examined in a blinded manner by a pathologist (TDO). Organs examined were the liver, lung, and kidney. A single microscopic section was examined from each mouse organ, so frequencies reported are a minimal estimate since organs were not serially sectioned.

For electron microscopic examination, two *Sod1*^{+/+} and three *Sod1*^{-/-} mice of both sexes were examined at 16 months. In *Sod1*^{-/-} mice, both tumors and tissue adjacent to tumors were analysed. Tissues submitted for electron microscopy were processed in a routine manner; liver tissues were fixed in glutaraldehyde, embedded in Epon, thin sections double stained with lead citrate and uranyl acetate, and examined in a H-600 Hitachi electron microscope.

Enzyme assays

Aconitase activities were determined as described previously with minor modifications (Huang *et al.*, 2002). Briefly, serial dilutions of each sample were separated on Cellogel[®] (300 μm thickness, Accurate Chemical & Scientific Corp., Westbury, NY, USA) at 130 V for 1 h in a potassium phosphate buffer (20 mM, pH 6.4) containing 3.7 mM citric acid. C-ACO and M-ACO were detected by activity staining of the gel (Huang *et al.*, 2002). The enzyme activities were determined as a function of the band intensity and quantitated with image analysis software GelExpert (Nucleotech, San Mateo, CA, USA).

MnSOD activities were determined on a non-denaturing IEF gel (Ampholine PAGplate pH 3.5–9.5, Amersham Pharmacia Biotech Inc., Piscataway, NJ, USA) as described previously (Huang *et al.*, 2002). Catalase and GPx activities were determined spectrophotometrically as described (Aebi, 1984; Flohe and Gunzler, 1984). All enzyme activities were calculated as band intensity or unit/mg protein. The values from *Sod1*^{-/-} mice were then normalized to that of age-matched *+/+* controls and expressed as the percentage of age-matched control. All chemicals and enzymes were purchased from Sigma (St Louis, MO, USA).

Western blot analyses

Liver C-ACO, M-ACO, MnSOD, CAIII, APEX1, cyclin D1, D2, and D3, porin, and Met were quantitated by Western blot analyses. Protein samples were separated by 4–20% SDS-PAGE (Readygels, Bio-Rad, Hercules, CA, USA) at 120 V for 90 min and transferred to nitrocellulose membranes. The nitrocellulose membranes were incubated in blocking buffer (5% nonfat dry milk in PBS and 0.05% Tween 20 (pH 7.4)) for 1 h followed sequentially by the primary antibody (1 h), wash (3 \times 15 min, PBS/0.05% Tween 20), HRP-conjugated secondary antibody (1 h), and wash (3 \times 15 min). Finally, the membranes were incubated with the ECL chemiluminescent reagent (Amersham Biosciences, Piscataway, NJ, USA) for 1 min and exposed to Lumifilm (Roche Applied Science, Indianapolis, IN, USA) for 30 s to 1 min to obtain optimal signal intensity. All procedures were carried out at room temperature.

The primary antibodies used in this study were the following: rabbit polyclonal antibodies – C-ACO and M-ACO (1:2000), University of Wisconsin (Chen *et al.*, 1997; Schalinske *et al.*, 1997); cyclin D2 (SC593, 1:330), Santa Cruz Biotechnology (Santa Cruz, CA, USA); and MnSOD (SOD111, 1:4000), Stressgen (Victoria, BC, Canada). The mouse monoclonal antibodies – cyclin D1 (SC246, 1:330), D3 (SC6283, 1:330), and Met (SC8057, 1:500), Santa Cruz Biotechnology; porin (529538, 1:500), Calbiochem (La Jolla, CA, USA); APEX1 (R610817, 1:500), BD Biosciences (San Jose, CA, USA); and actin (A 5441, 1:500), Sigma. Goat polyclonal antibody – CAIII (PA-4010, 1:10 000), Spectral Diagnostics (Toronto, Canada). The secondary antibodies used were as follows: HRP-goat anti-rabbit (SC2004, 1:2000) and HRP-rabbit anti-goat (SC2768, 1:2000), Santa Cruz Biotechnology; HRP-goat anti-mouse (172-1011, 1:5000), Bio-Rad. All primary and secondary antibodies were diluted in the blocking buffer except the antibody against Met. This antibody was blocked and diluted in the Detector Block Solution from KPL (Gaithersburg, MD, USA). All blots were stripped with the Western Blot Recycling Kit from Alpha Diagnostics (San Antonio, TX, USA) and reprobed with an antibody against actin as a loading control. Quantitation of Western blot results was carried out by first normalizing the protein level of each sample to that of actin. The ratio of normalized KO to control levels was then calculated.

The amounts of total proteins loaded were as follows: C-ACO, 10 μg for the *+/+* samples and 40 μg for the *-/-* samples; M-ACO, 20 μg each, MnSOD and CAIII, 15 μg each; cyclin D1, D2, D3, Met, porin, and APEX1, 60 μg each.

Immunohistochemistry analyses

Subcellular localization of APEX1 and 8-oxo dG was determined by IHC on paraffin-embedded liver sections. The sections were deparaffinized in xylene and hydrated through graded ethanol. Endogenous peroxidase was inactivated by treating the sections with 3% H_2O_2 and 0.1% Triton X-100 in PBST (150 mM Tris-HCl, 150 mM NaCl, and 0.05% Tween 20 (pH 7.6)) for 20 min. Antigen unmasking was carried out for APEX1 by boiling the sections in 600 ml 10 mM citric acid (pH 6) for 20 min and allowed to cool down to room temperature. For detecting DNA/RNA oxidation, sections were pretreated with proteinase K (20 $\mu g/ml$, 37°C, 40 min) followed by HCl (2 N, 20 min). However, *Sod1*^{-/-} sections often required a higher concentration of proteinase K (320 $\mu g/ml$) to obtain consistent IHC signals. The MOM basic kit (mouse-on-mouse, Vector Lab, Burlingame, CA, USA) was used to block nonspecific binding sites for 1 h. The sections were sequentially

washed in PBST (2×2 min) and MOM diluents (1×5 min), treated with primary antibody for 1 h (diluted in MOM diluents), washed in PBST (2×2 min), treated with biotinylated secondary antibody for 20 min, washed in PBST (2×2 min), treated with the VECTASTAIN ABC reagent (avidin and biotinylated HRP, Vector Lab) for 30 min, and washed in PBST (2×2 min). Immunostain was developed with diaminobenzidine (DAB kit, Vector Lab).

Mouse monoclonal antibodies for APEX1 (NB 100–116, Novus Biological, Littleton, CO, USA) and DNA/RNA oxidative damage markers (QED Bioscience, San Diego, CA, USA) and biotinylated anti-mouse secondary antibody (MOM kit, Vector Lab) were used at the dilution of 1:250, 1:1000, and 1:250, respectively. The antibody for DNA/RNA oxidative damage markers recognizes both oxidized DNA and RNA (Liu *et al.*, 2002). To distinguish between the two, sections were treated with RNase-free DNase I ($10 \text{ U}/\mu\text{l}$) or DNase-free RNase A ($10 \text{ mg}/\text{ml}$) at 37°C for 3 h after proteinase K and HCl treatments. Perhaps due to the higher levels of 8-oxo dG, *Sod1*^{-/-} sections usually required a longer (overnight) DNase I treatment for the nuclear signals to completely disappear.

Determination of oxidative DNA damage

Total DNA was isolated from livers using the NaI method as described (Hamilton *et al.*, 2001). The concentration of 8-oxo dG in the DNA hydrolysate was determined by HPLC using a CoulArray[®] electrochemical detection system (ESA Model 5500/5600, ESA Inc., Chelmsford, MA, USA) and a 150×4.6 C-18 column (YMC, Wilmington, NC, USA) (Hamilton *et al.*, 2001). The identities of 2 dG and 8-oxo dG on the chromatograms were determined by coinjection of standards. The standards were also run after every sixth sample for verification. The data are expressed as the ratio of nmol of 8-oxo dG to 10^5 nmol of 2 dG.

Determination of protein oxidation

The appearance of carbonyl groups in proteins can be used to detect and quantify oxidative modification of proteins (Levine *et al.*, 1994). The protein carbonyl contents in *Sod1*^{+/+}, *-/-*, *+/-*, and *-/-* liver tissue lysates were detected by the OxyBlot protein oxidation detection kit (S7150, Intergen, Purchase, NY, USA) with minor modification as per the manufacturer's instructions. To derivatize the carbonyl group for Western blot detection, equal volumes of tissue lysate (at $3 \mu\text{g}/\mu\text{l}$) and 12% SDS were mixed, followed by the addition of 2 volumes of 20 mM 2,4-DNPH (dinitrophenylhydrazine) in 10% trifluoroacetic acid. The mixture was incubated in the dark at room temperature for 20 min, and a neutralization solution (1.5 volumes) from the Oxyblot kit was added to stop the reaction. Nonderivatized controls were run for each sample. A total of

$15 \mu\text{g}$ protein from each sample was loaded in 4–20% gradient Readygel, and SDS-PAGE and Western blotting were performed according to the manufacturer's instructions. The primary antibody was a rabbit polyclonal antibody raised against DNP (dinitrophenylhydrazone, S7150-4, Intergen) and was used at 1:150 dilution. The HRP-conjugated secondary antibody (S7150-5, Intergen) was used at 1:300 dilution.

Analyses of lipid peroxidation

MDA and HAE levels were determined with a colorimetric method using the BIOXYTECH LPO-586 kit (Oxis Research, Portland, OR, USA). Tissues used for MDA and HAE analysis were homogenized in the presence of 5 mM butylated hydroxytoluene (BHT) to prevent further oxidation. The levels of F_2 -isoprostanes in liver samples were determined using gas chromatography/negative-ion chemical ionization/mass spectrometry (GC-NICI-MS) as described (Morrow and Roberts, 1999). Briefly, tissues (100–200 mg) were homogenized in ice-cold Folch solution (chloroform/methanol 2:1) containing 5 mg/100 ml BHT. Lipids were extracted and hydrolysed with 15% KOH. After acidification, the F_2 -isoprostanes were extracted with a C_{18} Sep-Pak column and a silica Sep-Pak column, converted to pentafluororobenzyl esters, and purified by thin-layer chromatography. The purified F_2 -isoprostanes were derivatized to trimethylsilyl ether derivatives and quantified by GC/MS using [³H]₄8-Iso-PGF_{2 α} as an internal standard. The amount of F_2 -isoprostanes is expressed as ng of 8-Iso-PGF_{2 α} /g of tissue.

Statistical analyses

Survival analysis was carried out with Kaplan–Meier survival analysis; ANOVA and Student's *t*-test were used for all other analyses. The statistical analysis program JMP (SAS Institutes, Inc., Cary, NC, USA) was used, and a *P*-value of ≤ 0.05 was considered significant.

Acknowledgements

We thank Anna Bogdanova and Xinli Wong for excellent animal care, Aaron Tward and Sanja Kakar for helpful discussion, and Charles Limoli for critical reading of the manuscript. This work was supported by funding from the Stanford Cancer Council (TTH), American Cancer Society (HVR), and the National Institutes of Health AG16633 (TTH), AG16998 (CJE), DK47219 (RSE), GM42056 (MERIT Award to LJR), GM15431 (LJR), and DK26657 (LJR), and resources and the use of facilities at the Palo Alto VA Health Care System, Palo Alto, CA (TTH) and the William S Middleton Memorial Veterans Administration Hospital, Madison, WI (TDO).

References

- Aebi H. (1984). *Methods Enzymol.*, **105**, 121–126.
- Agar JN, Krebs C, Frazzoon J, Huynh BH, Dean DR and Johnson MK. (2000). *Biochemistry*, **39**, 7856–7862.
- Anzenbacher P and Anzenbacherova E. (2001). *Cell Mol. Life Sci.*, **58**, 737–747.
- Asahi M, Fujii J, Suzuki K, Seo HG, Kuzuya T, Hori M, Tada M, Fujii S and Taniguchi N. (1995). *J. Biol. Chem.*, **270**, 21035–21039.
- Bai J, Zhu X, Zheng X and Wu Y. (1998). *Chin. Med. J. (Engl.)*, **111**, 789–792.
- Blum HE. (2002). *Dig. Dis.*, **20**, 81–90.

- Bobola MS, Blank A, Berger MS, Stevens BA and Silber JR. (2001). *Clin. Cancer Res.*, **7**, 3510–3518.
- Bonkovsky HL and Lambrecht RW. (2000). *Clin. Liver Dis.*, **4**, 409–429, vi–vii.
- Cabiscol E and Levine RL. (1995). *J. Biol. Chem.*, **270**, 14742–14747.
- Casari M, Corso F, Bassi A, Capra F, Gabrielli GB, Stanzial AM, Nicoli N and Corrocher R. (1994). *Int. J. Clin. Lab. Res.*, **24**, 94–97.
- Chang LY, Slot JW, Geuze HJ and Crapo JD. (1988). *J. Cell Biol.*, **107**, 2169–2179.

- Chen OS, Schalinske KL and Eisenstein RS. (1997). *J. Nutr.*, **127**, 238–248.
- Chisari FV, Klopchin K, Moriyama T, Pasquinelli C, Dunsford HA, Sell S, Pinkert CA, Brinster RL and Palmiter RD. (1989). *Cell*, **59**, 1145–1156.
- Court FG, Wemyss-Holden SA, Dennison AR and Maddern GJ. (2002). *Br. J. Surg.*, **89**, 1089–1095.
- Crapo JD, Oury T, Rabouille C, Slot JW, Chang LY and Geuze HJ. (1992). *Proc. Natl. Acad. Sci. USA*, **89**, 10405–10409.
- Crawford DH, Leggett BA and Powell LW. (1998). *Baillieres Clin. Gastroenterol.*, **12**, 209–225.
- Crichton RR, Wilmet S, Legssyer R and Ward RJ. (2002). *J. Inorg. Biochem.*, **91**, 9–18.
- Deane NG, Parker MA, Aramandla R, Diehl L, Lee WJ, Washington MK, Nanney LB, Shyr Y and Beauchamp RD. (2001). *Cancer Res.*, **61**, 5389–5395.
- Diehl AM. (2002). *Front. Biosci.*, **7**, e301–e314.
- Dominguez-Malagon H and Gaytan-Graham S. (2001). *Ultrastruct. Pathol.*, **25**, 497–516.
- Drapier JC. (1997). *Methods*, **11**, 319–329.
- Eisenstein RS. (2000). *Annu. Rev. Nutr.*, **20**, 627–662.
- Evans AR, Limp-Foster M and Kelley MR. (2000). *Mutat. Res.*, **461**, 83–108.
- Fletcher LM and Halliday JW. (2002). *J. Intern. Med.*, **251**, 181–192.
- Flint DH, Tuminello JF and Emptage MH. (1993). *J. Biol. Chem.*, **268**, 22369–22376.
- Flohe L and Gunzler WA. (1984). *Methods Enzymol.*, **105**, 114–121.
- Fridovich I. (1995). *Annu. Rev. Biochem.*, **64**, 97–112.
- Gardner PR. (1997). *Biosci. Rep.*, **17**, 33–42.
- Gardner PR and Fridovich I. (1991). *J. Biol. Chem.*, **266**, 19328–19333.
- Gardner PR, Raineri I, Epstein LB and White CW. (1995). *J. Biol. Chem.*, **270**, 13399–13405.
- Haddow JE, Palomaki GE, McClain M and Craig W. (2003). *J. Med. Screen.*, **10**, 11–13.
- Hamilton ML, Guo Z, Fuller CD, Van Remmen H, Ward WF, Austad SN, Troyer DA, Thompson I and Richardson A. (2001). *Nucleic Acids Res.*, **29**, 2117–2126.
- Hanigan MH, Kemp CJ, Ginsler JJ and Drinkwater NR. (1988). *Carcinogenesis*, **9**, 885–890.
- Huang C and Wu M. (1990). *Zhonghua Yi Xue Za Zhi*, **70**, 138–139, 12.
- Huang TT, Raineri I, Eggerding F and Epstein CJ. (2002). *Methods Enzymol.*, **349**, 191–213.
- Huang TT, Yasunami M, Carlson EJ, Gillespie AM, Reaume AG, Hoffman EK, Chan PH, Scott RW and Epstein CJ. (1997). *Arch. Biochem. Biophys.*, **344**, 424–432.
- Inagaki T, Katoh K, Takiya S, Ikuta K, Kobayashi S, Suzuki M, Fukuzawa Y, Ayakawa T, Shimizu K and Tagaya T. (1992). *Gastroenterol. Jpn.*, **27**, 382–389.
- Jaeschke H, Gores GJ, Cederbaum AI, Hinson JA, Pessayre D and Lemasters JJ. (2002). *Toxicol. Sci.*, **65**, 166–176.
- Keller GA, Warner TG, Steimer KS and Hallewell RA. (1991). *Proc. Natl. Acad. Sci. USA*, **88**, 7381–7385.
- Kennedy MC, Antholine WE and Beinert H. (1997). *J. Biol. Chem.*, **272**, 20340–20347.
- Kennedy MC and Beinert H. (1988). *J. Biol. Chem.*, **263**, 8194–8198.
- Kruidenier L, van Meeteren ME, Kuiper I, Jaarsma D, Lamers CB, Zijlstra FJ and Verspaget HW. (2003). *Free Radic. Biol. Med.*, **34**, 753–765.
- Kuo WH, Chiang WL, Yang SF, Yeh KT, Yeh CM, Hsieh YS and Chu SC. (2003). *Life Sci.*, **73**, 2211–2223.
- Lee GH, Nomura K, Kanda H, Kusakabe M, Yoshiki A, Sakakura T and Kitagawa T. (1991). *Cancer Res.*, **51**, 3257–3260.
- Lee GH, Nomura K and Kitagawa T. (1989). *Carcinogenesis*, **10**, 2227–2230.
- Lee HC, Li SH, Lin JC, Wu CC, Yeh DC and Wei YH. (2004). *Mutat. Res.*, **547**, 71–78.
- Levine RL. (2002). *Free Radic. Biol. Med.*, **32**, 790–796.
- Levine RL, Williams JA, Stadtman ER and Shacter E. (1994). *Methods Enzymol.*, **233**, 346–357.
- Levy L, Renard CA, Wei Y and Buendia MA. (2002). *Ann. NY Acad. Sci.*, **963**, 21–36.
- Liaw KY, Lee PH, Wu FC, Tsai JS and Lin-Shiau SY. (1997). *Am. J. Gastroenterol.*, **92**, 2260–2263.
- Lii CK, Chai YC, Zhao W, Thomas JA and Hendrich S. (1994). *Arch. Biochem. Biophys.*, **308**, 231–239.
- Lin MT, Wang MY, Liaw KY, Lee PH, Chien SF, Tsai JS and Lin-Shiau SY. (2001). *Hepatogastroenterology*, **48**, 1102–1105.
- Liu J, Head E, Gharib AM, Yuan W, Ingersoll RT, Hagen TM, Cotman CW and Ames BN. (2002). *Proc. Natl. Acad. Sci. USA*, **99**, 2356–2361.
- Liu Y and Liu G. (2004). *Biochem. Pharmacol.*, **67**, 777–785.
- Loeb LA. (1991). *Cancer Res.*, **51**, 3075–3079.
- Missirlis F, Hu J, Kirby K, Hilliker AJ, Rouault TA and Phillips JP. (2003). *J. Biol. Chem.*, **278**, 47365–47369, Epub 2003, Sep 12.
- Moriya K, Nakagawa K, Santa T, Shintani Y, Fujie H, Miyoshi H, Tsutsumi T, Miyazawa T, Ishibashi K, Horie T, Imai K, Todoroki T, Kimura S and Koike K. (2001). *Cancer Res.*, **61**, 4365–4370.
- Morrow JD and Roberts II LJ. (1999). *Methods Enzymol.*, **300**, 3–12.
- Murray CJ and Lopez AD. (1997). *Lancet*, **349**, 1436–1442.
- Muse KE, Oberley TD, Sempf JM and Oberley LW. (1994). *Histochem. J.*, **26**, 734–753.
- Neonaki M, Graham DC, White KN and Bomford A. (2002). *Biochem. Soc. Trans.*, **30**, 726–728.
- Nowell PC, Rowlands Jr DT, Daniele RP, Berger BM and Guerry D. (1979). *Clin. Immunol. Immunopathol.*, **12**, 323–330.
- Oberley LW. (2001). *Antioxid. Redox. Signal.*, **3**, 461–472.
- Oberley TD, Toyokuni S and Szweda LI. (1999). *Free Radic. Biol. Med.*, **27**, 695–703.
- Oberley TD, Zhong W, Szweda LI and Oberley LW. (2000). *Prostate*, **44**, 144–155.
- Olinski R, Gackowski D, Foksinski M, Rozalski R, Roszkowski K and Jaruga P. (2002). *Free Radic. Biol. Med.*, **33**, 192–200.
- Ozaki M, Suzuki S and Irani K. (2002). *FASEB J.*, **16**, 889–890.
- Perlmutter DH. (2000). *Clin. Liver Dis.*, **4**, 387–408, vi.
- Pigeolet E, Corbisier P, Houbion A, Lambert D, Michiels C, Raes M, Zachary MD and Remacle J. (1990). *Mech. Ageing Dev.*, **51**, 283–297.
- Pugh TD and Goldfarb S. (1992). *Cancer Res.*, **52**, 280–284.
- Puglisi F, Aprile G, Minisini AM, Barbone F, Cataldi P, Tell G, Kelley MR, Damante G, Beltrami CA, Di Loreto C, Robertson KA, Bullock HA, Xu Y, Tritt R, Zimmerman E, Ulbright TM, Foster RS and Einhorn LH. (2001). *Anticancer Res.*, **21**, 4041–4049.
- Raisanen SR, Lehenkari P, Tasanen M, Rahkila P, Harkonen PL and Vaananen HK. (1999). *FASEB J.*, **13**, 513–522.
- Robertson KA, Bullock HA, Xu Y, Tritt R, Zimmerman E, Ulbright TM, Foster RS, Einhorn LH and Kelley MR. (2001). *Cancer Res.*, **61**, 2220–2225.

- Rosenwald IB, Kaspar R, Rousseau D, Gehrke L, Leboulch P, Chen JJ, Schmidt EV, Sonenberg N and London IM. (1995). *J. Biol. Chem.*, **270**, 21176–21180.
- Sauer H, Neukirchen W, Rahimi G, Grunheck F, Hescheler J and Wartenberg M. (2004). *Exp. Cell Res.*, **294**, 313–324.
- Schalinske KL, Blemings KP, Steffen DW, Chen OS and Eisenstein RS. (1997). *Proc. Natl. Acad. Sci. USA*, **94**, 10681–10686.
- Shringarpure R and Davies KJ. (2002). *Free Radic. Biol. Med.*, **32**, 1084–1089.
- Shringarpure R, Grune T and Davies KJ. (2001). *Cell Mol. Life Sci.*, **58**, 1442–1450.
- Sola B, Salaun V, Ballet JJ and Troussard X. (1999). *Int. J. Cancer*, **83**, 230–234.
- Sturtz LA, Diekert K, Jensen LT, Lill R and Culotta VC. (2001). *J. Biol. Chem.*, **276**, 38084–38089, Epub 2001, Aug 10.
- Sun Y, Oberley LW, Oberley TD, Elwell JH and Sierra-Rivera E. (1993). *Carcinogenesis*, **14**, 1457–1463.
- Takahashi M, Dinse GE, Foley JF, Hardisty JF and Maronpot RR. (2002). *Toxicol. Pathol.*, **30**, 599–605.
- Valgimigli M, Valgimigli L, Trere D, Gaiani S, Pedulli GF, Gramantieri L and Bolondi L. (2002). *Free Radic. Res.*, **36**, 939–948.
- Wallace SS. (2002). *Free Radic. Biol. Med.*, **33**, 1–14.
- Wang R, Ferrell LD, Faouzi S, Maher JJ and Bishop JM. (2001). *J. Cell Biol.*, **153**, 1023–1034.
- Yu DY, Moon HB, Son JK, Jeong S, Yu SL, Yoon H, Han YM, Lee CS, Park JS, Lee CH, Hyun BH, Murakami S and Lee KK. (1999). *J. Hepatol.*, **31**, 123–132.
- Zhang Y, Zhao W, Zhang HJ, Domann FE and Oberley LW. (2002). *Cancer Res.*, **62**, 1205–1212.
- Zimmermann A. (2002). *Med. Sci. Monit.*, **8**, RA53–RA63.

Supplementary Information accompanies the paper on Oncogene website (<http://www.nature.com/onc>).